network

MDPI

Article

Polar Codes with Differential Phase Shift Keying for Selective Detect-and-Forward Multi-Way Relaying Systems

Ruilin Ji † and Harry Leib *

Department of Electrical and Computer Engineering, McGill University, Montreal, QC H3A 0E9, Canada; ruilin.ji@mail.mcgill.ca

* Correspondence: harry.leib@mcgill.ca

† Current address: Department of Electrical and Computer Engineering, McMaster University, Hamilton, ON L8S 4L8, Canada.

Abstract: Relaying with network coding forms a basis for a variety of collaborative communication systems. A linear block coding framework for multi-way relaying using network codes introduced in the literature shows great promise for understanding, analyzing, and designing such systems. So far, this technique has been used with low-density parity check (LDPC) codes and belief propagation (BP) decoding. Polar codes have drawn significant interest in recent years because of their low decoding complexity and good performance. Our paper considers the use of polar codes also as network codes with differential binary phase shift keying (DBPSK), bypassing the need for channel state estimation in multi-way selective detect-and-forward (DetF) cooperative relaying. We demonstrate that polar codes are suitable for such applications. The encoding and decoding complexity of such systems for linear block codes is analyzed using maximum likelihood (ML) decoding for LDPC codes with log-BP decoding and polar codes with successive cancellation (SC) as well as successive cancellation list (SCL) decoding. We present Monte-Carlo simulation results for the performance of such a multi-way relaying system, employing polar codes with different lengths and code rates. The results demonstrate a significant performance gain compared to an uncoded scheme. The simulation results show that the error performance of such a system employing polar codes is comparable to LDPC codes with log-BP decoding, while the decoding complexity is much lower. Furthermore, we consider a hard threshold technique at user terminals for determining whether a relay transmits or not. This technique makes the system practical without increasing the complexity and can significantly reduce the degradation from intermittent relay transmissions that is associated with such a multi-way relaying protocol.

Keywords: cooperative communication systems; polar codes; relaying systems; network codes; channel codes

check for updates

Citation: Ji, R.; Leib, H. Polar Codes with Differential Phase Shift Keying for Selective Detect-and-Forward Multi-Way Relaying Systems. *Network* **2024**, *4*, 313–337. https://doi.org/10.3390/network4030015

Academic Editor: Martin Reisslein

Received: 12 June 2024
Revised: 30 July 2024
Accepted: 31 July 2024
Published: 8 August 2024

Copyright: © 2024 by the authors. Licensee MDPI, Basel, Switzerland. This article is an open access article distributed under the terms and conditions of the Creative Commons Attribution (CC BY) license (https://creativecommons.org/licenses/by/4.0/).

1. Introduction

Cooperative communication is an important paradigm for improving the operation and performance of wireless telecommunication networks [1–5]. Relaying techniques are principal enablers for cooperative communication, which are commonly used in wireless systems [6–9]. In such systems, user terminal (source) nodes transmit information carrying signals to the relays and the destination nodes. The relay nodes then forward information related signals to the destination following specific protocols. Finally, destination nodes decode the information from user terminal based on the signals received from these terminals and relay nodes. With the aid of relays that provide additional paths for information transmission, the error performance and power efficiency of such systems is improved compared to non-cooperative schemes [10]. Common protocols for relaying systems are broadly classified into amplify-and-forward (AF) and decode-and-forward (DF) methods [11]. With the AF protocol, the relays amplify the received signals from the terminals

and forward them to the destination. In the DF protocol, the relays first decode the signals from the terminals and extract the information, which is then re-encoded and forwarded to the destination. Detect-and-forward (DetF) relaying, considered in Zhang and Leib [7] as well as in Hou and Leib [12], is closely related to DF, except that each relay only detects (demodulates) the signal, without decoding. These protocols are further classified into selective AF and selective DF techniques [13], where the relays operate selectively on the signals received from the terminals according to specific criteria. Using selective techniques, the performance is improved over conventional all-participation relaying [14].

Network coding, first proposed by Ahlswede [15], requires computation within the network. In a network-coded system, intermediate nodes form and transmit functions of the information they receive; a technique that can improve throughput. Network coding has found many applications in modern communication networks [16] as well as in cooperative communication [17,18]. Furthermore, network coding serves as a basis for many relaying protocols [19,20]. Three-node two-way relay networks (TWRNs) are a simple model of a cooperative communication system. In TWRNs, two terminals exchange information with the aid of one relay. In traditional TWRNs, a full information exchange cycle requires four phases, where each terminal consumes one phase to transmit to the relay and other terminal, then the relay consumes two phases to transmit to each of the two terminals. With network coding, the transmission is reduced to three phases, where the relay requires only one phase to transmit the properly combined data [7,21] to both terminals. This model can be further generalized to multi-way relay networks (MWRNs) [10,22], where multiple terminals exchange information with the aid of multiple relays. A linear block-coding framework for network-coded MWRNs with differential modulation that is based on systematic codes has been proposed in [12], which addresses the use of low-density parity check (LDPC) codes in systematic form as network codes. Decoding has been performed using the Belief Propagation (BP) algorithm. A simpler alternative is offered by systematic equivalent polar codes used as network codes for MWRNs, which is the main subject of the present paper.

Polar codes were first proposed by Arikan [23] and have drawn increasing research interest [24]. Polar codes are linear block codes that can achieve capacity over binary-input discrete memoryless channels (B-DMC). Compared with other advanced codes such as Turbo codes [25] and LDPC codes [26], polar codes have the advantage of lower encoding and decoding complexities with successive cancellation (SC) decoding. Furthermore, polar codes are more flexible in rate-adaptation, meaning that changing the number of information bits given a fixed codeword length will not affect the encoder structure. Polar codes have been widely used in communication systems, including 5G networks and beyond [27–29]. One disadvantage of polar codes is that when the codeword length is not long enough, the error performance with SC decoding is mediocre. Successive cancellation list (SCL) decoding for polar codes was proposed in Tal and Vardi [30] for improving error rate performance. The use of polar codes in relaying systems has been considered in [31–34]. The original polar codes are non-systematic and therefore not suitable for the MWRN of [12]. The first systematic polar encoding algorithm was proposed by Arikan [35]. Most research on systematic polar encoding has focused on the implementation and optimization of this algorithm [36–38]. A modified systematic encoding method was proposed by Sarkis et al. [39,40], where the information bits are preserved at the input of the encoder. However, the above approaches mainly focus on reducing the encoding complexity, and none of the encoding functions are implemented by directly using a systematic generator matrix as required in the MWRN system of [12]. Therefore, an appropriate systematic encoding method of polar codes needs to be devised in order to make polar codes suitable for the MWRN system of [12].

This paper considers polar codes with Differential Binary Phase Shift Keying (DBPSK) modulation for MWRN. Compared to similar relaying systems employing LDPC codes, polar codes reduce the decoding complexity while still maintaining a comparable error performance. In this paper, we show how to employ systematic equivalent polar codes in MWRN and present the corresponding SC and SCL decoding algorithms for such systems.

Then we analyze and compare the encoding and decoding complexity with maximum likelihood (ML) decoding for any linear block code, for LDPC codes with log-BP decoding, and for polar codes with SC and SCL decoding. While many other decoding techniques exist for polar codes [24,41–47], in this paper, we choose to consider the classical SC and SCL algorithms, providing results that can be used as benchmarks when considering other techniques. Because of the selective DetF relaying protocol used in MWRNs, the relays transmit intermittently. Different transmission cases are considered based on whether the terminals know which relays transmit or not. Simulation results show that MWRNs with polar codes provide significant gain compared to uncoded schemes. For short polar codes, the error performance is compared with ML decoding. For longer polar codes, the performance is compared with LDPC codes with log-BP decoding. The rest of this paper is organized as follows. Section 2 introduces the system model and analyzes the encoding and decoding complexity with ML decoding and LDPC codes with log-BP decoding. Section 3 demonstrates how to employ systematic equivalent polar codes in MWRN with DBPSK and analyzes the corresponding decoding complexity. Section 4 presents performance simulation results of MWRN employing polar codes and a comparison with ML decoding, as well as with LDPC codes using log-BP decoding. Section 5 presents the conclusions.

2. System Model and Complexity Analysis

For readers' convenience, Table 1 provides a list of symbols used in this paper with their definitions.

Table 1. Table of main symbols.

Symbol	Definition
T_k	k-th user terminal
R_l	l-th relay
$\mathcal{S}$	Set of terminals and relays
m_i	Information symbol with values in $\{0, 1\}$
$a_i[k]$	BPSK symbol with values in $\{1, -1\}$
$b_i[k]$	Differentially encoded symbol with values in $\{1, -1\}$
f_ij	Channel coefficient from node i to node j
$y_ij[k]$	Received signal at node j from node i
n_ij	Noise samples in the channel from node i to node j
N_0	Variance in additive channel noise
E_b	Bit energy
P_i	Transmission power of node i
$\varphi_{ij}[k]$	Phase of $y_{ij}[k]y_{ij}^*[k-1]$
$\theta_i[k]$	Phase of $a_i[k]$
$\theta_n[k]$	Phase noise term affecting the decision variable
$\mathbf{G}_{sys}$	Systematic generator matrix of a linear block code
$\mathbf{G}_{nonsys}$	Nonsystematic generator matrix of a linear block code
$\mathbf{P}_{K\times L}$	Parity submatrix of a systematic generator matrix
$I(W)$	Symmetric capacity of channel W
$W(y\|x)$	Transition probabilities of a channel
$Z(W)$	Bhattacharyya parameter of channel W
$W_N^{(i)}$	i-th synthesized channel from a collection of N channels

Table 1. *Cont.*

Symbol	Definition
$\mathbf{G}_N$	Encoding matrix of a length N polar code
$\mathbf{F}$	Basic submatrix of a polar code encoding matrix
$\mathbf{G}_A$	Submatrix of $\mathbf{G}_N$ that contains all the rows with indices in $\mathcal{A}$
$L_N^{(i)}(\cdot,\cdot)$	Log likelihood ratio (LLR) for bit channel i
$\mathrm{PM}_l^{(i)}$	Path metric of the l-th candidate at bit i
$\mathbf{G}_A p$	Resulting matrix from permuting the columns of $\mathbf{G}_A$
$\mathbf{G}_{AA}$	Submatrix of $\mathbf{G}_A p$ of elements $G_{i,j}$ of $\mathbf{G}_N$ with $i \in \mathcal{A}, j \in \mathcal{A}$
$\mathcal{CN}(\cdot,\cdot)$	Complex normal (Gaussian) distribution

2.1. A Linear Block Coding Framework for Multi-Way Relaying

Consider a wireless system with K user terminals denoted by $T_1, T_2, \ldots, T_K$ and L relays denoted by $R_1, R_2, \ldots R_L$ as in ref. [12]. The transmission protocol of the system is based on time division multiple access, and it is presented in Table 2. Each node in the system operates in half-duplex mode and consumes one phase to transmit one symbol in one transmission time slot. Each relay is associated with a relevant group of user terminals whose information symbols are used to form the symbol forwarded by the relay. The relays utilize the selective DetF protocol, which means that a relay will forward the combined signal from its relevant group of terminals only if it correctly detects all the signals received from the terminals in its relevant group. Otherwise, the relay will remain silent. The set of all nodes is denoted by $\mathcal{S} = \{T_1, T_2, \ldots, T_K, R_1, R_2, \ldots, R_L\}$. When $1 \leq i \leq K$, the ith node of $\mathcal{S}$ is T_i. When $K+1 \leq i \leq K+L$, the ith node of $\mathcal{S}$ is R_{i-K}.

Table 2. Transmission protocol used in this system.

	Transmitter	Receiver
Phase 1	T_1	$T_2, \ldots, T_K, R_1, R_2, \ldots, R_L$
Phase 2	T_2	$T_1, T_3, \ldots, T_K, R_1, R_2, \ldots, R_L$
...	...	...
Phase K	T_K	$T_1, \ldots, T_{K-1}, R_1, R_2, \ldots, R_L$
Phase $K+1$	R_1	$T_1, T_2, \ldots, T_K$
Phase $K+2$	R_2	$T_1, T_2, \ldots, T_K$
...	...	...
Phase $K+L$	R_L	$T_1, T_2, \ldots, T_K$

One transmission time slot is composed of $N = K + L$ phases. The relation between the transmission time slots and phases is presented in Figure 1. During the first K phases in a time slot, each terminal T_i broadcasts its own information symbol to all L relays $R_1, R_2, \ldots R_L$ and $K-1$ terminals $T_1, \ldots T_{i-1}, T_{i+1} \ldots, T_K$. During the subsequent L phases, every relay utilizes the selective DetF protocol to transmit a combined signal from its relevant group to the other $K-1$ terminals. Hence, complete exchange of one information symbol from all terminals including relay forwardings is achieved during a single time slot. All nodes employ DBPSK; hence, channel state information (CSI) is not required for decoding. The information symbol vector is denoted by $\mathbf{m} = (m_1, m_2, \ldots, m_{K+L})$, where $m_i \in \{0, 1\}$ is the information symbol transmitted by node i. The BPSK symbol at node i at time slot k is denoted by $a_i[k]$, which can be represented as follows:

$$a_i[k] = 1 - 2m_i[k], k \in \mathbb{Z} \quad (1)$$

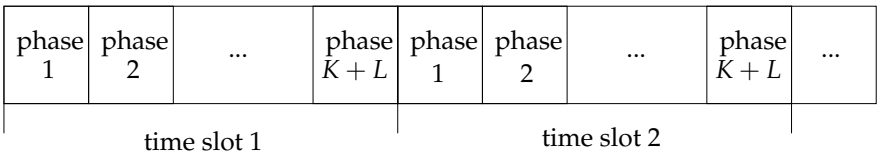

Figure 1. Relation between transmission time slots and phases.

Hence, $a_i[k] \in \{1, -1\}$. After differential encoding, the corresponding DBPSK symbol is as follows:

$$b_i[k] = a_i[k]b_i[k-1] \tag{2}$$

In this paper, we denote the channel coefficient from node i to node j by f_{ij}. Furthermore, we assume that all channels are reciprocal quasi-static [48] and hence $f_{ij} = f_{ji}$ following the Rayleigh model. This represents slow rate fading, where the channels remain constant over a time slot. However, they change independently between different time slots. With Rayleigh fading, f_{ij} are zero-mean circularly symmetric complex Gaussian (CSCG) with normalized power $E\{|f_{ij}|^2\} = 1$. Then, the received signal at node j from node i is as follows:

$$y_{ij}[k] = \sqrt{P_i} f_{ij} b_i[k] + n_{ij}[k] \tag{3}$$

where the noise samples $n_{ij}[\cdot]$ are uncorrelated zero-mean CSCG with variance $\sigma_n^2 = N_0$, and P_i is the transmission power of node i. All the nodes in the system are assumed to use the same transmission power.

In this work, we assume the relays know whether a detected symbol is correct, as in [49]. Practical techniques that can be used to achieve such conditions are discussed in [50]. The relays employ conventional differential detection (CDD) to demodulate the received signals from the terminals. Using CDD, the symbols are detected based on the phase of $y_{ij}[k]y_{ij}^*[k-1]$. The phase of $y_{ij}[k]y_{ij}^*[k-1]$ is denoted by $\varphi_{ij}[k]$, and the phase of $a_i[k]$ is denoted by $\theta_i[k]$, where $\theta_i[k] = 0$ or π for BPSK. Based on (2) and (3),

$$\begin{aligned} y_{ij}[k]y_{ij}^*[k-1] &= (\sqrt{P_i} f_{ij} b_i[k] + n_{ij}[k])(\sqrt{P_i} f_{ij}^* b_i^*[k-1] + n_{ij}^*[k-1]) \\ &= P_i |f_{ij}|^2 a_i[k] + \sqrt{P_i} f_{ij} b_i[k] n_{ij}^*[k-1] + \sqrt{P_i} f_{ij}^* b_i^*[k-1] n_{ij}[k] + n_{ij}[k] n_{ij}^*[k-1] \\ &= P_i |f_{ij}|^2 e^{j\theta_i[k]} + \sqrt{P_i} f_{ij} b_i[k] n_{ij}^*[k-1] + \sqrt{P_i} f_{ij}^* b_i^*[k-1] n_{ij}[k] + n_{ij}[k] n_{ij}^*[k-1] \\ &= |y_{ij}[k]y_{ij}^*[k-1]| e^{j\varphi_{ij}[k]} \end{aligned} \tag{4}$$

where

$$\varphi_{ij}[k] = \theta_i[k] + \theta_n[k] \tag{5}$$

and $\theta_n[k]$ is the phase noise due to the following term:

$$\sqrt{P_i} f_{ij} b_i[k] n_{ij}^*[k-1] + \sqrt{P_i} f_{ij}^* b_i^*[k-1] n_{ij}[k] + n_{ij}[k] n_{ij}^*[k-1].$$

Hence the detection decision rule for the received symbol from node i at node j is as follows:

$$\hat{m}_i[k] = \begin{cases} 0 & \text{if } -\pi/2 \le \varphi_{ij}[k] < \pi/2 \\ 1 & \text{otherwise} \end{cases} \tag{6}$$

If a relay R_l correctly detects all the symbols from all the terminals in its relevant group, then it will perform a binary linear combination of the corresponding symbols using a parity check column from a systematic generator matrix. The combined signal will be transmitted to all the terminals at transmission phase $K + l$. If R_l fails to detect all the symbols correctly, it will remain silent at phase $K + l$, and the terminals will receive only noise.

2.2. Linear Block Code Representation of the Multi-Way Relaying System

Based on [12], this scheme can be represented by a $(K+L, K)$ binary linear block code with a systematic generator matrix:

$$\mathbf{G}_{sys} = \begin{bmatrix} \mathbf{I}_{K\times K} & \mathbf{P}_{K\times L} \end{bmatrix} = \begin{bmatrix} 1 & 0 & \cdots & 0 & p_{1,1} & p_{1,2} & \cdots & p_{1,L} \\ 0 & 1 & \cdots & 0 & p_{2,1} & p_{2,2} & \cdots & p_{2,L} \\ \vdots & \vdots & \ddots & \vdots & \vdots & \vdots & \ddots & \vdots \\ 0 & 0 & \ldots & 1 & p_{K,1} & p_{K,2} & \cdots & p_{K,L} \end{bmatrix} \tag{7}$$

where the identity matrix $\mathbf{I}_{K\times K}$ corresponds to the first K phases involving user-to-user transmissions, and and the parity check submatrix $\mathbf{P}_{K\times L}$ corresponds to the subsequent L phases involving network-coded transmissions from relays. The element at the ith row and jth column of $\mathbf{P}$ is denoted by $P_{i,j}$, which can assume the values 0 or 1. The elements 1 on the jth column of $\mathbf{P}$ correspond to the terminals in the relevant group of R_j (i.e., T_i is in the relevant group of R_j if $P_{i,j} = 1$).

The codeword of one transmission time slot is denoted by $\mathbf{x} = (x_1, x_2, \ldots, x_{K+L})$, and the information bits from the terminals are denoted by $\mathbf{m}_T = (m_1, m_2, \ldots, m_K)$. With all operations performed in the binary field $\mathbb{GF}(2)$, the vectors $\mathbf{x}$ and $\mathbf{m}_T$ are related by the following:

$$\mathbf{x} = \mathbf{m}_T \mathbf{G}_{sys} = (\mathbf{m}_T, \mathbf{m}_T \mathbf{P}) \tag{8}$$

Therefore, for $1 \leq j \leq K$, $x_j = m_j$. For $K+1 \leq j \leq K+L$,

$$x_j = \sum_{i=1}^{K} P_{i,j} m_i. \tag{9}$$

2.3. Maximum Likelihood (ML) Decoding

At terminal node j, a ML decoder for DBPSK employs the decision rule [12]:

$$\hat{\mathbf{c}} = \underset{\mathbf{c}}{\text{argmax}} p(\mathbf{y}_j[k] | \mathbf{c}, \mathbf{y}_j[k-1]) \tag{10}$$

where $\mathbf{y}_j[k] = (y_{1j}[k], y_{2j}[k], \ldots, y_{Nj}[k])$, $\mathbf{y}_j[k-1] = (y_{1j}[k-1], y_{2j}[k-1], \ldots, y_{Nj}[k-1])$ and $\mathbf{c} = (a_1[k], a_2[k], \ldots, a_N[k])$. In our system, all transmissions are independent over independent channels; thus, for the modulated symbols $a_i[k]$ and $b_i[k-1]$, the channel fading coefficient f_{ij} and noise samples $n_{ij}[k]$ are all independent for different nodes i. Thus, $y_{1j}[k], y_{2j}[k], \ldots, y_{Nj}[k]$ are independent. Therefore,

$$\begin{aligned} p(\mathbf{y}_j[k] | \mathbf{c}, \mathbf{y}_j[k-1]) &= p(y_{1j}[k], \ldots, y_{Nj}[k] | a_1[k], \ldots, a_N[k], y_{1j}[k-1], \ldots, y_{Nj}[k-1]) \\ &= \prod_{i=1}^{N} p(y_{ij}[k] | a_1[k], \ldots, a_N[k], y_{1j}[k-1], \ldots, y_{Nj}[k-1]) \\ &= \prod_{i=1}^{N} p(y_{ij}[k] | a_i[k], y_{ij}[k-1]) \end{aligned} \tag{11}$$

where $y_{ij}[k]$ only depends on $a_i[k]$ and $y_{ij}[k-1]$.

Furthermore, we have the following:

$$\begin{aligned} p(y_{ij}[k] | a_i[k], y_{ij}[k-1]) &= \frac{p(y_{ij}[k], a_i[k], y_{ij}[k-1])}{p(a_i[k], y_{ij}[k-1])} \\ &= \frac{p(y_{ij}[k], a_i[k], y_{ij}[k-1]) / p(a_i[k])}{p(a_i[k], y_{ij}[k-1] / p(a_i[k]))} \\ &= \frac{p(y_{ij}[k], y_{ij}[k-1] | a_i[k])}{p(y_{ij}[k-1] | a_i[k])} = \frac{p(y_{ij}[k], y_{ij}[k-1] | a_i[k])}{p(y_{ij}[k-1])} \end{aligned} \tag{12}$$

where $y_{ij}[k-1]$ does not depend on $a_i[k]$.

Using (10) to (12), we have the following:

$$\begin{aligned}\hat{\mathbf{c}} &= \underset{\mathbf{c}}{\operatorname{argmax}} p(\mathbf{y}_j[k]|\mathbf{c}, \mathbf{y}_j[k-1]) = \underset{\mathbf{c}}{\operatorname{argmax}} \prod_{i=1}^{N} \frac{p(y_{ij}[k], y_{ij}[k-1]|a_i[k])}{p(y_{ij}[k-1])} \\ &= \underset{\mathbf{c}}{\operatorname{argmax}} \prod_{i=1}^{N} p(y_{ij}[k], y_{ij}[k-1]|a_i[k])\end{aligned} \tag{13}$$

where $p(y_{ij}[k-1])$ does not depend on the choice of $\mathbf{c}$. Using similar derivation steps to those in [12], and given the fact that in our system, $a_i[k]$ are real, we obtain the final ML decoding metric for DBPSK:

$$\hat{\mathbf{c}} = \underset{\mathbf{c}}{\operatorname{argmax}} \sum_{i=1}^{N} a_i[k](y_{ij}^*[k]y_{ij}[k-1] + y_{ij}[k]y_{ij}^*[k-1]) \tag{14}$$

2.4. Complexity Analysis for General Linear Block Codes and LDPC Codes

In this section, we analyze the complexity of encoding and decoding at each node. The complexity is measured by the number of basic operations that one algorithm consumes to encode or decode a codeword. Decoding complexities of different algorithms are compared by calculating the number of basic operations an algorithm employs for decoding one codeword at a node. In some cases, we use the order of magnitude $O(\cdot)$ complexity metric when considering the asymptotic behavior for large systems.

Assume a linear block code. In our system, the encoding process is performed using a systematic generator matrix. For a (N, K) systematic linear block code, the encoding process is equivalent to the multiplication of a $1 \times K$ information vector by a $K \times N$ generator matrix. The total complexity of this operation is $O(KN)$. However, in our system, the encoding process is performed by N nodes, and each node only calculates one bit of a codeword. The terminals transmit one information symbol to the other nodes, and there are no other calculations. For relay nodes, the CDD calculation (4) for one node involves a complex multiplication with complexity $O(1)$. Consider the worst case, when the relevant group sizes associated with the relays approach the maximal value K. In this case, each relay performs K CDDs and $K-1$ binary additions of the K detected symbols. Therefore, the encoding complexity for relay nodes is $O(K)$.

Next, we analyze the number of different operations required at each terminal node with ML decoding and LDPC codes with log-BP decoding. Calculating the sign function or comparing two real numbers is regarded as one comparison operation. Looking up one number or value from a existing table is regarded as one table look-up operation. Multiplying a number by 1 or –1 is not considered as a multiplication in the following analysis.

When using ML decoding with (14), two multiplications and one addition are needed to calculate one term in the summation; hence, $2N$ multiplications and $N + N - 1 = 2N - 1$ additions are required for the summation corresponding to one codeword. For a (N, K) linear block code, there are a total of 2^K possible codewords. Their value are pre-stored in a table; hence, there are a total of 2^K table look-ups of codewords, $2^{K+1}N$ multiplications, and $2^K(2N-1)$ additions. Finally, finding the codeword that maximizes the summation in (14) requires 2^K comparisons. We see the exponential dependency on K in the complexity results for ML decoding of general linear block codes, which poses a significant challenge for long codes of non-vanishing small rates.

We now assume an LDPC code with average variable node degree distribution d_v and average check node distribution d_c. The number of operations required at each step for binary LDPC codes with log-BP decoding is presented in Table 3, where I_{max} is the maximum number of iterations. The steps are divided based on the descriptions in [12]. The number of operations required for updating the variables $L(q_{uv}(z))$ and $L(r_{uv}(z))$ are analyzed in [51], and the results are summarized in Table 3. Calculating tentative LLR

for each symbol in $x[k]$ is similar to updating $L(q_{uv}(z))$, which involves Ld_cd_v additions. Then, making tentative decisions for each symbol requires N comparisons. Finally, $\hat{\mathbf{x}} \cdot \mathbf{H}$ is calculated to determine whether to stop the iterations. This requires $N(d_c)$ multiplications, $N(d_c - 1)$ additions, and table look-ups of non-zero elements of $\mathbf{H}$. To achieve a better error performance, I_{max} needs to be set to a relatively large value, resulting in a high decoding complexity.

Table 3. Number of operations at each step of low-density parity check (LDPC) codes with log-belief propagation (BP) decoding.

	Multiplication	**Addition**	**Comparison**	**Table Look-Up**
Initialization	$3N$	$2N$	-	-
Update $L(r_{uv}(z))$	-	$6(3d_c - 4)LI_{max}$	$2(3d_c - 4)LI_{max}$	$2(3d_c - 4)LI_{max}$
Update $L(q_{uv}(z))$	-	$Ld_c(d_v - 1)I_{max}$	-	-
Tentative LLRs	-	$Ld_cd_vI_{max}$	NI_{max}	-
$\hat{\mathbf{x}} \cdot \mathbf{H}^T$	Nd_cI_{max}	$N(d_c - 1)I_{max}$	-	NLI_{max}

In Table 3, we notice the terms composed of four-factor multiplications involved in the number of additions required to update $L(q_{uv}(z))$ and to calculate tentative LLRs. These contribute significantly to increasing complexity in LDPC decoding. Next, we consider polar codes for our multi-way relaying system, analyze complexity, and compare them with the results of the LDPC codes.

3. Polar Codes for the Multi-Way Relaying System

3.1. Background on Polar Codes

Let $W : \mathcal{X} \to \mathcal{Y}$ be a binary-input discrete memoryless channel (B-DMC) with input and output alphabets $\mathcal{X} = \{0, 1\}$ and $\mathcal{Y} = \mathbb{R}$ (the set of real numbers), respectively. The transition probability of the channel is denoted by $W(y|x)$, where $x \in \mathcal{X}, y \in \mathcal{Y}$. Let the subvector $(m_i, \ldots m_j)$ of $\mathbf{m}$ be denoted by $\mathbf{m}_i^j$. If $i > j$, then $\boldsymbol{m}_i^j$ is the null vector.

There are two parameters that indicate the channel quality for polar codes: the symmetric capacity $I(W)$ and the Bhattacharyya parameter $Z(W)$. These are defined in [23] as follows:

$$I(W) = \sum_{y \in \mathcal{Y}} \sum_{x \in \mathcal{X}} \frac{1}{2} W(y|x) \log \frac{W(y|x)}{\frac{1}{2}W(y|0) + \frac{1}{2}W(y|1)} \tag{15}$$

$$Z(W) = \sum_{y \in Y} \sqrt{W(y|0)W(y|1)} \tag{16}$$

where the logarithm is taken with a basis of 2. The symmetric capacity $I(W)$ is the highest rate for reliable communication with equal input probabilities, and the Bhattacharyya parameter $Z(W)$ is an upper bound to the error probability under ML decoding when transmitting over W. It was shown in [23] that for any B-DMC, the following two inequalities hold:

$$I(W) \geq \log \frac{2}{1 + Z(W)} \tag{17}$$

$$I(W) \leq \sqrt{1 - Z(W)^2} \tag{18}$$

Based on (17) and (18), $I(W) \approx 1$ iff $Z(W) \approx 0$, which indicates that the channel is reliable.

Polar codes exploit the channel polarization phenomenon. In channel polarization, N independent copies of a B-DMC employing channel combining and channel splitting are

transformed into N synthesized bit channels $\{W_N^{(i)} : 1 \leq i \leq N\}$, where $W_N^{(i)}$ denotes the i-th such synthesized channel. As N tends to infinity, the symmetric capacity $I(W_N^{(i)})$ tends towards 0 or 1; hence, it is polarized. The transition probability of the ith bit channel $W_N^{(i)}$ is as follows [23]:

$$W_N^{(i)}(\mathbf{y}_1^N, \mathbf{m}_1^{i-1} | m_i) = \sum_{\mathbf{m}_{i+1}^N} \frac{1}{2^{N-1}} W_N(\mathbf{y}_1^N | \mathbf{m}_1^N) \tag{19}$$

For an (N, K) polar code, the information bits are arranged to be located at the K most reliable bit locations and are transmitted over the best K bit channels. The other $N - K$ bits are called frozen bits, and their values are known to the decoder. Frozen bits do not carry information and are set to fixed values. In this work, all frozen bits are set to 0. The process of selecting the information bit indices of polar codes is called the construction of polar codes.

We define set $\mathcal{A}$ as the collection of all information bit indices of a polar code. We denote the information bits of the polar code by $\mathbf{m}_A$ and the frozen bits by $\mathbf{m}_{A^c}$. The encoding matrix of a (N, K) polar code is as follows [23]:

$$\mathbf{G}_N = \mathbf{F}^{\otimes \log_2 N} \tag{20}$$

where $\mathbf{F} = \begin{bmatrix} 1 & 0 \\ 1 & 1 \end{bmatrix}$ is the fundamental building matrix (called the kernel matrix), and $\otimes n$ denotes the nth-fold Kronecker product of a matrix.

Using operations performed over the binary field $\mathbb{GF}(2)$, we can express the original polar encoded codeword as follows:

$$\mathbf{x} = \mathbf{m}\mathbf{G}_N = \mathbf{m}_A \mathbf{G}_A + \mathbf{m}_{A^c} \mathbf{G}_{\mathcal{A}^c} \tag{21}$$

where $\mathbf{G}_A$ is the submatrix of $\mathbf{G}_N$ that contains all the rows of $\mathbf{G}_N$ with indices in $\mathcal{A}$, $\mathbf{G}_{\mathcal{A}^c}$ is the submatrix of $\mathbf{G}_N$ that contains all the rows of $\mathbf{G}_N$ with indices in $\mathcal{A}^c$, and $\mathbf{m}$ is an input vector containing information bits and frozen bits. When all the frozen bits are set to 0, (21) becomes:

$$\mathbf{x} = \mathbf{m}_A \mathbf{G}_A \tag{22}$$

showing that $\mathbf{G}_A$ is the generator matrix. When encoding with (22), $\mathbf{m}_A$ does not appear in the resultant codeword $\mathbf{x}$; thus, the original polar codes are non-systematic and cannot be used for our multi-way relaying system. $\mathbf{G}_{nonsys} \triangleq \mathbf{G}_A$ is defined as the non-systematic generator matrix of polar codes.

As an example, consider an $(8, 5)$ polar code with frozen bits set $\mathcal{A}^c = \{1, 2, 3\}$ and information bits set $\mathcal{A} = \{4, 5, 6, 7, 8\}$. The polar encoding for this code is shown in Figure 2. The encoding process of an (N, K) polar code consists of $\log_2 N + 1$ stages denoted by $S_0, S_1, S_2 \ldots S_{\log_2 N}$. The input to the encoder $\mathbf{m}$ is at S_0. At each subsequent stage, there are $N/2 = 4$ binary additions. For this $(8, 5)$ polar code,

$$\mathbf{G}_N = \mathbf{F}^{\otimes 3} = \begin{bmatrix} \mathbf{F} & 0 & 0 & 0 \\ \mathbf{F} & \mathbf{F} & 0 & 0 \\ \mathbf{F} & 0 & \mathbf{F} & 0 \\ \mathbf{F} & \mathbf{F} & \mathbf{F} & \mathbf{F} \end{bmatrix} = \begin{bmatrix} 1 & 0 & 0 & 0 & 0 & 0 & 0 & 0 \\ 1 & 1 & 0 & 0 & 0 & 0 & 0 & 0 \\ 1 & 0 & 1 & 0 & 0 & 0 & 0 & 0 \\ 1 & 1 & 1 & 1 & 0 & 0 & 0 & 0 \\ 1 & 0 & 0 & 0 & 1 & 0 & 0 & 0 \\ 1 & 1 & 0 & 0 & 1 & 1 & 0 & 0 \\ 1 & 0 & 1 & 0 & 1 & 0 & 1 & 0 \\ 1 & 1 & 1 & 1 & 1 & 1 & 1 & 1 \end{bmatrix} \tag{23}$$

The nonsystematic generator matrix $\mathbf{G}_{nonsys}$ selects the rows in $\mathcal{A}$ of $\mathbf{G}_N$, i.e., the last five rows to transmit information bits:

$$\mathbf{G}_{nonsys} = \begin{bmatrix} 1 & 1 & 1 & 1 & 0 & 0 & 0 & 0 \\ 1 & 0 & 0 & 0 & 1 & 0 & 0 & 0 \\ 1 & 1 & 0 & 0 & 1 & 1 & 0 & 0 \\ 1 & 0 & 1 & 0 & 1 & 0 & 1 & 0 \\ 1 & 1 & 1 & 1 & 1 & 1 & 1 & 1 \end{bmatrix} \tag{24}$$

Reed–Muller (RM) codes [52] are closely related to polar codes. Both codes with codeword length N use the same matrix $\mathbf{G}_N$ for code construction. While the generator matrix of polar codes selects the most reliable rows with the lowest error probabilities of $\mathbf{G}_N$ based on the specific channel and SNR, the generator matrix of (r, n) RM codes with order r and codeword length $N = 2^n$ selects the rows of $\mathbf{G}_N$ with Hamming weights $w \geq 2^{n-r}$. Equivalently, polar codes freeze the least-reliable channels, while RM codes freeze the channels with the lowest Hamming weights. Consequently, polar codes have a better error performance, since the code design is channel-specific to improve error performance, while RM codes have a higher minimum Hamming distance.

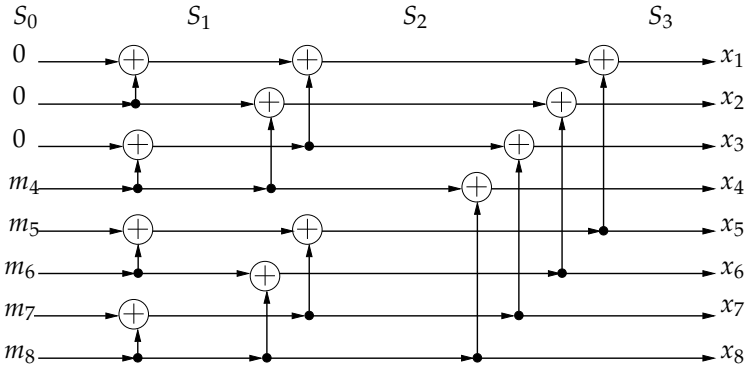

Figure 2. Encoder of a $(8, 5)$ polar code.

The Log likelihood ratio (LLR) for the ith bit channel is given by the following:

$$L_N^{(i)}(\mathbf{y}, \hat{\mathbf{m}}_1^{i-1}) \triangleq \ln \frac{W_N^{(i)}(\mathbf{y}, \hat{\mathbf{m}}_1^{i-1} | m_i = 0)}{W_N^{(i)}(\mathbf{y}, \hat{\mathbf{m}}_1^{i-1} | m_i = 1)} \tag{25}$$

With SC decoding, each bit is decoded successively from m_1 to m_N. The decoder employs the following decision rule for the ith bit:

$$\hat{m}_i = \begin{cases} 0 & \text{if } i \in \mathcal{A}^c \\ 0 & \text{if } L_N^{(i)}(\mathbf{y}, \hat{\mathbf{m}}_1^{i-1}) \geq 0, i \in \mathcal{A} \\ 1 & \text{if } L_N^{(i)}(\mathbf{y}, \hat{\mathbf{m}}_1^{i-1}) < 0, i \in \mathcal{A} \end{cases} \tag{26}$$

The calculation of (25) can be performed recursively in the log domain [53]:

$$\begin{aligned} L_N^{(2i-1)}(\mathbf{y}_1^N, \hat{\mathbf{m}}_1^{2i-2}) \approx \operatorname{sign}(L_{N/2}^{(i)}(\mathbf{y}_1^{N/2}, \hat{\mathbf{m}}_{1,o}^{2i-2} + \hat{\mathbf{m}}_{1,e}^{2i-2})) \cdot \operatorname{sign}(L_{N/2}^{(i)}(\mathbf{y}_{N/2+1}^N, \hat{\mathbf{m}}_{1,e}^{2i-2})) \\ \cdot \min(|L_{N/2}^{(i)}(\mathbf{y}_1^{N/2}, \hat{\mathbf{m}}_{1,o}^{2i-2} + \hat{\mathbf{m}}_{1,e}^{2i-2})|, |L_{N/2}^{(i)}(\mathbf{y}_{N/2+1}^N, \hat{\mathbf{m}}_{1,e}^{2i-2})|) \end{aligned} \tag{27}$$

$$L_N^{(2i)}(\mathbf{y}_1^N, \hat{\mathbf{m}}_1^{2i-1}) = (1 - 2\hat{m}_{2i-1})[L_{N/2}^{(i)}(\mathbf{y}_1^{N/2}, \hat{\mathbf{m}}_{1,o}^{2i-2} + \hat{\mathbf{m}}_{1,e}^{2i-2})] + L_{N/2}^{(i)}(\mathbf{y}_{N/2+1}^N, \hat{\mathbf{m}}_{1,e}^{2i-2}) \tag{28}$$

where $\mathbf{m}_{1,o}^{2i-2}$ is the subvector of $\mathbf{m}_1^{2i-2}$ with odd indices,and $\mathbf{m}_{1,e}^{2i-2}$ is the subvector of $\mathbf{m}_1^{2i-2}$ with even indices. The recursion continues until we reach the calculation of LLR of $W_1^{(1)}$. In this case,

$$L_1^{(1)}(y_i) = \ln \frac{W(y_i|0)}{W(y_i|1)} \tag{29}$$

is called the channel LLR, which can be calculated from the channel. A more detailed description of SC decoding can be found in [23].

The SCL algorithm is a modified version of SC decoding and follows a similar serial decoding process from m_1 to m_N. While SC decoding only considers the best decoding result, SCL decoding forms a list of L_{max} best possible decoding results. The decoding result in the SCL algorithm is named as a candidate path having a path metric. In the log domain, the path metric PM of the lth candidate path at the ith bit is defined as follows [54]:

$$\mathrm{PM}_l^{(\mathrm{i})} = -\ln p(\hat{\mathbf{m}}_1^i|\hat{\mathbf{y}}_1^N) = \sum_{j=1}^{i} \ln(1 + e^{-(1-2\hat{m}_j)L_N^{(j)}}) \tag{30}$$

A smaller path metric corresponds to a higher $p(\hat{\mathbf{m}}_1^i|\hat{\mathbf{y}}_1^N)$, which indicates a higher likelihood for that candidate path. The updating rule of the path metric at bit index i is as follows:

$$\mathrm{PM}_l^{(\mathrm{i})} = \begin{cases} \mathrm{PM}_l^{(\mathrm{i}-1)} & \text{if } \hat{m}_i = \frac{1}{2}(1 - \mathrm{sign}(L_N^{(i)})) \\ \mathrm{PM}_l^{(\mathrm{i}-1)} + |L_N^{(i)}| & \text{otherwise} \end{cases} \tag{31}$$

Equation (31) indicates that if the decoding result of list l for bit i does not coincide with the corresponding LLR, then a penalty $|L_N^{(k)}|$ is added to the path metric.

Before decoding m_1, the initial path metrics are all set to 0. When decoding a frozen bit, the value 0 is appended to all candidate paths, and the path metrics are updated. When decoding an information bit m_i, instead of making a hard decision using (26), the SCL decoder appends both possible decoding results of 0 or 1 to the identical copies of the current decoding candidates, which doubles the number of active candidate paths. When the number of candidate paths exceeds L_{max}, only the L_{max} candidate paths with the lowest path metrics are kept, and others are pruned. After decoding m_N, the active candidate path with the lowest path metric is selected to be the final decoding result. By using a lazy-copy technique to duplicate the candidate paths, the decoding complexity of SCL decoding is $O(L_{max}N\log N)$ [30].

3.2. Systematic Polar Encoding for the Multi-Way Relaying System

For any non-systematic linear block code with generator matrix $\mathbf{G}_{nonsys}$, there exists a systematic equivalent code with systematic generator matrix $\mathbf{G}_{sys}$ [55], satisfying the following relation:

$$\mathbf{G}_{nonsys} = \mathbf{B}\mathbf{G}_{sys} \tag{32}$$

where $\mathbf{B}$ is a $K \times K$ invertible matrix. A code and its systematic equivalent form have the same codewords. Only the mappings of the information vector to codewords are different. These mappings are related through a linear reversible transformation represented by the matrix $\mathbf{B}$ of (32).

We define $\mathbf{G}_{AA}$ as the $K \times K$ submatrix of $\mathbf{G}_N$ of (20) that consists of elements $G_{i,j}$ with $i \in \mathcal{A}, j \in \mathcal{A}$. The matrix $\mathbf{G}_N$ is lower triangular with diagonal elements $G_{d,d} = 1$, $1 \leq d \leq N$. The diagonal elements of $\mathbf{G}_{AA}$ are $G_{i,i}$ with $i \in \mathcal{A}$, which are also diagonal elements of $\mathbf{G}_N$. Therefore, the diagonal elements of $\mathbf{G}_{AA}$ are also all equal to 1, and $\mathbf{G}_{AA}$ is invertible. The systematic encoder in [35] chooses $\mathbf{B} = \mathbf{G}_{AA}$. However, with this selection, the information bits are located at all bit indices in $\mathcal{A}$ of the codeword $\mathbf{x}$, which we denote as $\mathbf{x}_A$. In our system, the bits transmitted by the terminals $\mathbf{m}_T$ are located at the first K bit indices of $\mathbf{x}$. Therefore, the columns of $\mathbf{G}_A$ are first permuted before the construction of the

equivalent systematic generator matrix. We define the resultant matrix from permuting the columns of $\mathbf{G}_A$ as $\mathbf{G}_{Ap}$, which has the following form:

$$\mathbf{G}_{Ap} = \begin{bmatrix} \mathbf{G}_{AA} & \mathbf{G}_{AA^c} \end{bmatrix} \tag{33}$$

where $\mathbf{G}_{AA^c}$ is a $K \times L$ submatrix of $\mathbf{G}_N$ that consists of all elements $G_{i,j}$ with $i \in \mathcal{A}, j \in \mathcal{A}^c$. The systematic generator matrix of the system is formed as follows:

$$\mathbf{G}_{sys} = \mathbf{G}_{AA}^{-1}\mathbf{G}_{Ap} = \mathbf{G}_{AA}^{-1}\begin{bmatrix} \mathbf{G}_{AA} & \mathbf{G}_{AA^c} \end{bmatrix} = \begin{bmatrix} \mathbf{I}_{K\times K} & \mathbf{G}_{AA}^{-1}\mathbf{G}_{AA^c} \end{bmatrix} = \begin{bmatrix} \mathbf{I}_{K\times K} & \mathbf{P}_{K\times L} \end{bmatrix} \tag{34}$$

The codeword $\mathbf{x}$ can be obtained from either $\mathbf{m}_T$ or $\mathbf{m}_A$:

$$\mathbf{x} = \mathbf{m}_T\mathbf{G}_{sys} = \mathbf{m}_A\mathbf{G}_{Ap} = \mathbf{m}_A\mathbf{G}_{AA}\mathbf{G}_{sys} \tag{35}$$

Therefore, the information bits transmitted by the terminals, $\mathbf{m}_T$, and the information bits of the original non-systematic polar code, $\mathbf{m}_A$, are related by the following:

$$\mathbf{m}_T = \mathbf{m}_A\mathbf{G}_{AA} \tag{36}$$

Encoding at the terminals is performed using $\mathbf{m}_T$, while polar decoding retrieves $\mathbf{m}_A$. However, after $\mathbf{m}_A$ is recovered using the SC or SCL algorithm, $\mathbf{m}_T$ can be obtained from (36). Notice that (36) can also be viewed as an encoding of $\mathbf{m}_A$ using the generator matrix $\mathbf{G}_{AA}$, which can be implemented recursively as in polar encoding.

3.3. Polar Decoding of the Multi-Way Relaying System

At each terminal receiver, the received symbols in one time slot are first reversely permuted to make the input order consistent with the non-systematic polar code required by SC or SCL decoders. The input channel LLRs of the decoder are calculated as follows:

$$\begin{aligned} L(y_{ij}^{'}[k]) &= \ln\frac{p(y_{ij}^{'}[k]|y_{ij}^{'}[k-1], x_i[k]=0)}{p(y_{ij}^{'}[k]|y_{ij}^{'}[k-1], x_i[k]=1)} \\ &= \ln\frac{p(y_{ij}^{'}[k], y_{ij}^{'}[k-1]|x_i[k]=0)/p(y_{ij}^{'}[k-1]|x_i[k]=0)}{p(y_{ij}^{'}[k], y_{ij}^{'}[k-1]|x_i[k]=1)/p(y_{ij}^{'}[k-1]|x_i[k]=1)} \\ &= \ln\frac{p(y_{ij}^{'}[k], y_{ij}^{'}[k-1]|x_i[k]=0)/p(y_{ij}^{'}[k-1])}{p(y_{ij}^{'}[k], y_{ij}^{'}[k-1]|x_i[k]=1)/p(y_{ij}^{'}[k-1])} \\ &= \ln\frac{p(y_{ij}^{'}[k], y_{ij}^{'}[k-1]|x_i[k]=0)}{p(y_{ij}^{'}[k], y_{ij}^{'}[k-1]|x_i[k]=1)} = \ln\frac{p(y_{ij}^{'}[k], y_{ij}^{'}[k-1]|a_i[k]=1)}{p(y_{ij}^{'}[k], y_{ij}^{'}[k-1]|a_i[k]=-1)} \end{aligned} \tag{37}$$

where $p(y_{ij}^{'}[k-1])$ does not depend on $p(x_i[k])$; thus, $p(y_{ij}^{'}[k-1]|x_i[k]) = p(y_{ij}^{'}[k-1])$.

The conditional PDF $p(y_{ij}^{'}[k], y_{ij}^{'}[k-1]|a_i[k])$ follows a multivariate complex Gaussian distribution when $a_i[k]$ is known, and it has the following form [56]:

$$\begin{aligned} p(y_{ij}^{'}[k], &y_{ij}^{'}[k-1]|a_i[k]) = \\ &\frac{1}{\pi^2(2P_i\sigma_n^2+\sigma_n^4)}\exp\{-\frac{1}{2P_i\sigma_n^2+\sigma_n^4}[(P_i+\sigma_n^2)(|y_{ij}^{'}[k]|^2+|y_{ij}^{'}[k-1]|^2) \\ &- P_i a_i[k](y_{ij}^{*'}[k]y_{ij}^{'}[k-1] + y_{ij}^{'}[k]y_{ij}^{*'}[k-1])]\} \end{aligned} \tag{38}$$

In the log domain,

$$\begin{aligned}&\ln(p(y_{ij}^{'}[k], y_{ij}^{'}[k-1]|a_i[k]))\\&= \ln[\frac{1}{\pi^2(2P_i\sigma_n^2+\sigma_n^4)}] - \frac{1}{2P_i\sigma_n^2+\sigma_n^4}[(P_i+\sigma_n^2)(|y_{ij}^{'}[k]|^2+|y_{ij}^{'}[k-1]|^2)\\&- P_i a_i[k](y_{ij}^{*'}[k]y_{ij}^{'}[k-1]+y_{ij}^{'}[k]y_{ij}^{*'}[k-1])]\end{aligned} \tag{39}$$

Therefore, the channel LLRs in (37) can be written as follows:

$$\begin{aligned}L(y_{ij}^{'}[k]) &= \ln(p(y_{ij}^{'}[k], y_{ij}^{'}[k-1]|a_i[k]=1)) - \ln(p(y_{ij}^{'}[k], y_{ij}^{'}[k-1]|a_i[k]=-1))\\&= \frac{1}{2P_i\sigma_n^2+\sigma_n^4}[P_i(1-(-1))(y_{ij}^{*'}[k]y_{ij}^{'}[k-1]+y_{ij}^{'}[k]y_{ij}^{*'}[k-1])]\\&= \frac{2P_i}{2P_i\sigma_n^2+\sigma_n^4}[(y_{ij}^{*'}[k]y_{ij}^{'}[k-1]+y_{ij}^{'}[k]y_{ij}^{*'}[k-1])]\end{aligned} \tag{40}$$

The LLR becomes

$$\begin{aligned}&\ln\frac{p(y_{ij}^{'}[k]|y_{ij}^{'}[k-1], x_i[k]=0)}{p(y_{ij}^{'}[k]|y_{ij}^{'}[k-1], x_i[k]=1)} = \ln\frac{p(y_{ij}^{'}[k], y_{ij}^{'}[k-1]|x_i[k]=0)}{p(y_{ij}^{'}[k], y_{ij}^{'}[k-1]|x_i[k]=1)}\\&= \ln\frac{p(y_{ij}^{'}[k], y_{ij}^{'}[k-1]|m_i[k]=0)}{p(y_{ij}^{'}[k], y_{ij}^{'}[k-1]|m_i[k]=1)}\\&= \ln\frac{p(y_{ij}^{'}[k], y_{ij}^{'}[k-1]|m_i[k]=0)p(m_i[k]=0)/p(y_{ij}^{'}[k], y_{ij}^{'}[k-1])}{p(y_{ij}^{'}[k], y_{ij}^{'}[k-1]|m_i[k]=1)p(m_i[k]=1)/p(y_{ij}^{'}[k], y_{ij}^{'}[k-1])}\\&= \ln\frac{p(m_i[k]=0|y_{ij}^{'}[k], y_{ij}^{'}[k-1])}{p(m_i[k]=1|y_{ij}^{'}[k], y_{ij}^{'}[k-1])}\end{aligned} \tag{41}$$

Each terminal T_i knows its own information bit $m_i[k]$; thus, when $m_i[k]=0$,

$$\ln\frac{p(y_{ij}^{'}[k]|y_{ij}^{'}[k-1], x_i[k]=0)}{p(y_{ij}^{'}[k]|y_{ij}^{'}[k-1], x_i[k]=1)} = \ln\frac{1}{0} = \infty \tag{42}$$

Similarly when $m_i[k]=1$,

$$\ln\frac{p(y_{ij}^{'}[k]|y_{ij}^{'}[k-1], x_i[k]=0)}{p(y_{ij}^{'}[k]|y_{ij}^{'}[k-1], x_i[k]=1)} = \ln\frac{0}{1} = -\infty \tag{43}$$

Therefore, the decoder at T_i sets the channel LLR corresponding to $m_i[k]$ to the following:

$$L(y_{ij}^{'}[k]) = \begin{cases}\infty & \text{if } m_i[k]=0\\ -\infty & \text{if } m_i[k]=1\end{cases} \tag{44}$$

In the simulations, the positive infinity and negative infinity in (44) are set to 10^{12} and 10^{-12}, respectively.

Next, we consider the channel LLRs for the silent relays. In our system, if a relay detects a wrong symbol and does not transmit, the terminals will receive only noise; hence, this sample should not be taken into account in the decoding process. This idea is encapsulated by the notion of the erasure channel. The basic binary erasure channel (BEC) model [23] is shown in Figure 3. The transition probabilities of BEC are given by $W(0|0) = W(1|1) = 1-p, W(\varepsilon|0) = W(\varepsilon|1) = p$, where ε is the erasure symbol. In general, if the received signal is unreliable and hence cannot be demodulated properly,

then the receiver declares an erasure denoted by a specific symbol, ε. In our system, an erasure corresponds to the event that a relay remains silent and hence the terminal receives only noise.

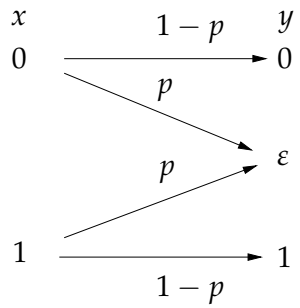

Figure 3. BEC channel model.

Since $p(y_{ij}[k] = \varepsilon | y_{ij}[k-1], x_i[k] = 0) = p(y_{ij}[k] = \varepsilon | y_{ij}[k-1], x_i[k] = 1)$, the corresponding channel LLR is set to the following:

$$L(y_{ij}^{'}[k]) = \ln \frac{p(y_{ij}^{'}[k] = \varepsilon | y_{ij}^{'}[k-1], x_i[k] = 0)}{p(y_{ij}^{'}[k] = \varepsilon | y_{ij}^{'}[k-1], x_i[k] = 1)} = \ln 1 = 0 \tag{45}$$

Hence, such a sample does not influence the decoding process.

The polar decoding process for the multi-way relaying system is summarized as follows [57]:

a. Reversely permute the received signal vector $\mathbf{y}$ into $\mathbf{y}^{'}$ based on π^{-1}.
b. Calculate channel LLRs $L(y_{ij}^{'}[k])$ according to (40) and (45).
c. Perform SC or SCL decoding of polar codes to recover $\hat{\mathbf{m}}_A$.
d. Obtain $\hat{\mathbf{m}}_T$ from $\hat{\mathbf{m}}_A$ using (36) implemented recursively through polar encoding.

3.4. Complexity Analysis of Polar Codes and Comparison

The encoding process of polar codes in the MWRN considered in this work is identical to the process described in Section 2; thus, the encoding complexity is the same. For the decoding process, each terminal first performs a reverse permutation of the received signal vector $\mathbf{y}$. The complexity of the reverse permutation is $O(N)$. Since we use the original SC and SCL decoders, the complexities of SC and SCL decoding in our system are still $O(N\log N)$ [23] and $O(L_{max}N\log N)$ [30]. For the final polar re-encoding process, we use the recursive structure of polar encoding, which has a complexity of $O(N\log N)$. In summary, the total decoding complexity at each terminal is $O(N\log N)$ for SC decoding and $O(L_{max}N\log N)$ for SCL decoding. The complexity at each node when employing polar codes is presented in Table 4.

Table 4. Complexity at each node when employing polar codes.

	Encoding	**Decoding**
Terminal	-	$O(N\log N)$ for SC, $O(L_{max}N\log N)$ for SCL
Relay	$O(K)$	-

Next, we analyze the number of required operations at each step for polar codes with SC decoding. The indices used for the reverse permutation are pre-stored in a table; thus, the reverse permutation step only requires N table look-ups. Calculating one channel LLR using (40) requires three multiplications and two additions; thus, calculating the total N channel LLRs requires $3N$ multiplications and $2N$ additions. According to (27), each term requires three comparisons and one multiplication, and each term in (28) requires one

comparison and one addition. There are $N/2\log_2 N$ terms; hence, (27) requires $N/2\log_2 N$ multiplications and $3N/2\log_2 N$ additions, and (28) requires $N/2\log_2 N$ multiplications and $N/2\log_2 N$ additions in total. The bit decision step in (26) requires N table look-ups to check whether the bit is frozen and K LLR comparisons for the decision of information bits. The re-encoding process consists of $\log_2 N$ stages. At each stage, there are $N/2$ additions. The total number of operations of each step for SC decoding is summarized in Table 5. For SCL decoding, the number of operations is related to the location of frozen bits and the path metrics, which is about L_{max} times of SC decoding.

The total number of required operations for polar codes with ML and SC decoding, as well as LDPC codes with log-BP decoding, is summarized in Table 6. For example, a $(512, 416)$ polar code requires 3840 multiplications and 5632 additions to decode a codeword using the SC technique. The $(437, 361)$ LDPC code in [12] has $d_c = 20$ and $d_v = 3.48$. When ignoring the operations in the initializations, the log-BP decoder requires 8740 multiplications and 42,898 additions for one iteration. This indicates that even when $I_{max} = 1$, the total number of operations required by polar codes with SC decoding is much lower than that of LDPC codes with log-BP decoding. The SC decoding complexity behaves as $N\log_2 N$, which in general, is lower than the complexities of the other two algorithms, log-BP and ML. Therefore, the low decoding complexity of polar codes make them attractive for MWRN applications.

Table 5. Number of operations at each step of successive cancellation (SC) decoding for the multi-way relaying system.

	Multiplication	**Addition**	**Comparison**	**Table Look-Up**
Reverse permutation	-	-	-	N
Channel LLRs	$3N$	$2N$	-	-
(27)	$N/2\log_2 N$	-	$3N/2\log_2 N$	-
(28)	-	$N/2\log_2 N$	$N/2\log_2 N$	-
Bit decision	-	-	K	N
Re-encoding	-	$N/2\log_2 N$	-	-

Table 6. Number of operations for different decoding techniques in the multi-way relaying system.

	Multiplication	**Addition**	**Comparison**	**Table Look-Up**
ML	$2^{K+1}N$	$2^K(2N-1)$	2^K	2^K
SC	$3N + N/2\log_2 N$	$N(2+\log_2 N)$	$2N\log_2 N + K$	$2N$
log-BP	$N(3 + d_c I_{max})$	$[L(2d_c d_v + 17d_c - 24) + N(d_c - 1)]I_{max} + 2N$	$(2(3d_c - 4)L + N)I_{max}$	$(2(3d_c - 4) + N)LI_{max}$

3.5. A Hard Threshold Technique at the Terminals

In practice, it is not possible for a terminal to know whether a relay transmits. In ref. [12], a hard threshold method at the terminals is proposed to overcome this problem. A terminal will consider a relay as active if the magnitude of the received signal passes the threshold. This can be cast as a binary hypothesis testing problem on the received sample Y at the terminal:

$$\begin{aligned} H_1 &: Y \sim \mathcal{CN}(0, P_i + N_0), \\ H_0 &: Y \sim \mathcal{CN}(0, N_0). \end{aligned} \tag{46}$$

The corresponding likelihood ratio test is as follows:

$$\Lambda = \frac{p_{Y|H_1}(y|H_1)}{p_{Y|H_0}(y|H_0)} \underset{H_0}{\overset{H_1}{\gtrless}} \mu \tag{47}$$

The probability of correct detection is denoted by $P_d = \{\Lambda > \mu | H_1\}$, and the probability of a false alarm is denoted by $P_f = \{\Lambda > \mu | H_0\}$. In [58], it is shown that the threshold μ that maximizes $(P_d - P_f)$ is $\mu = 1$. Ref. [12] shows that this test becomes the following when simplified:

$$|Y| \underset{H_0}{\overset{H_1}{\gtrless}} \sqrt{(N_0 + \frac{N_0^2}{P_i}) \ln(\frac{P_i}{N_0} + 1)} \triangleq \zeta \tag{48}$$

We consider a similar technique adapted for our MWRN with polar codes. In our system, if the received signal from a relay does not pass the threshold ζ, then the channel output most likely consists only of noise, indicating that the corresponding relay is silent. Hence, in this case, the signal at the terminal is interpreted as an erasure for decoding purposes, and the corresponding LLR $L(y'_{ij}[k])$ is taken as in (45). The receiver algorithm with the hard threshold for our system is presented in Figure 4.

At each terminal, comparing the received signals from all the relays with the hard threshold requires a complexity of $O(L)$. Hence, adding the threshold does not affect the decoding process complexity. Therefore, when employing the threshold method, the complexity is still $O(N\log N)$ for SC decoding and $O(L_{max} N\log N)$ for SCL decoding at each terminal.

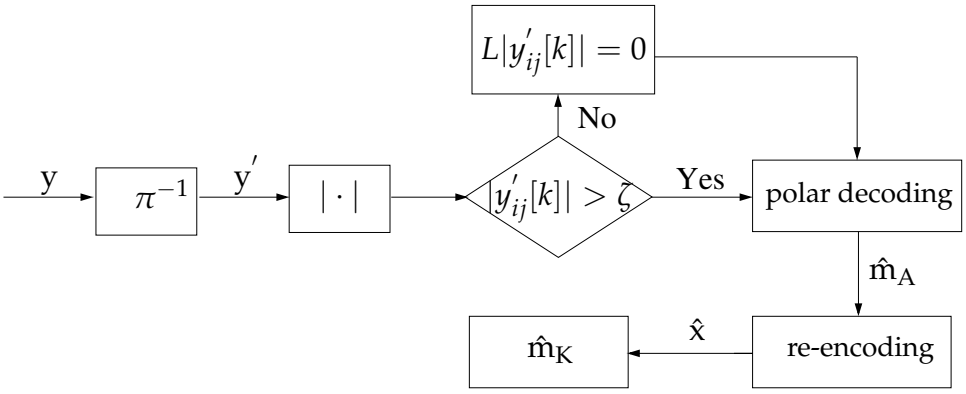

Figure 4. Receiver model of the terminals with the hard threshold.

4. Simulation Settings and Results

A performance analysis of our system with polar codes is conducted using extensive Monte-Carlo simulations implemented in MATLAB (version 2019).

4.1. Construction of Polar Codes

For computer simulations, we use the modified Monte-Carlo method from [59] to construct polar codes. At each designed E_b/N_0, we transmit 10^9 all-zero codewords over a quasi-static Rayleigh fading channel and decode the codewords with polar SC decoding. Since polar codes are linear codes, this can be viewed as treating all bits as frozen bits. With all-zero codewords, the encoding step can be omitted, and the decoding process is simplified. As the decoding proceeds, if bit m_i is decoded incorrectly as 1, we record an error at bit index i and correct it to 0. Then the decoding process continues. We collect the errors of each bit index from 1 to N at each E_b/N_0, and the L bit indices with the largest numbers of errors are selected to be the frozen bit indices. This ensures that the frozen bits indices correspond to least-reliable bits.

4.2. Testing the SC and SCL Decoders

To verify the correct operation of the SC and SCL decoders, we first reproduce the decoding results of [60]. That system employs a $(1024, 512)$ polar code constructed using frozen bit indices, as suggested for 5G [61]. The verification procedure is conducted over AWGN channels with quadrature phase shift keying (QPSK) modulation. Each QPSK symbol s carries two information bits. The additive noise samples are uncorrelated zero

mean CSCG random variables with variance σ_n^2 . The two information bits correspond to the symbols b_1 and b_2. We define sets $\mathcal{S}_i(0)$ and $\mathcal{S}_i(1)$, $i = 1$ or 2 of QPSK symbols as corresponding to information bits $b_i = 0$ or $b_i = 1$, respectively. The channel LLR for b_i is calculated as in [62]:

$$L(b_i) = \ln \frac{p(y|b_i = 0)}{p(y|b_i = 1)} = \ln \frac{\sum_{s \in \mathcal{S}_i(0)} e^{-\frac{|y-s|^2}{\sigma_n^2}}}{\sum_{s \in \mathcal{S}_i(1)} e^{-\frac{|y-s|^2}{\sigma_n^2}}}, i = 1, 2 \tag{49}$$

In Figure 5, we present the frame error rate (FER) performance of the $(1024, 512)$ polar code with SC and SCL decoding. Compared with the corresponding results from [60], which we also include in Figure 5 for convenience, we see a good match. Our simulation results are consistent with the results in [60], indicating that our implementations for the SC and SCL decoders operate correctly.

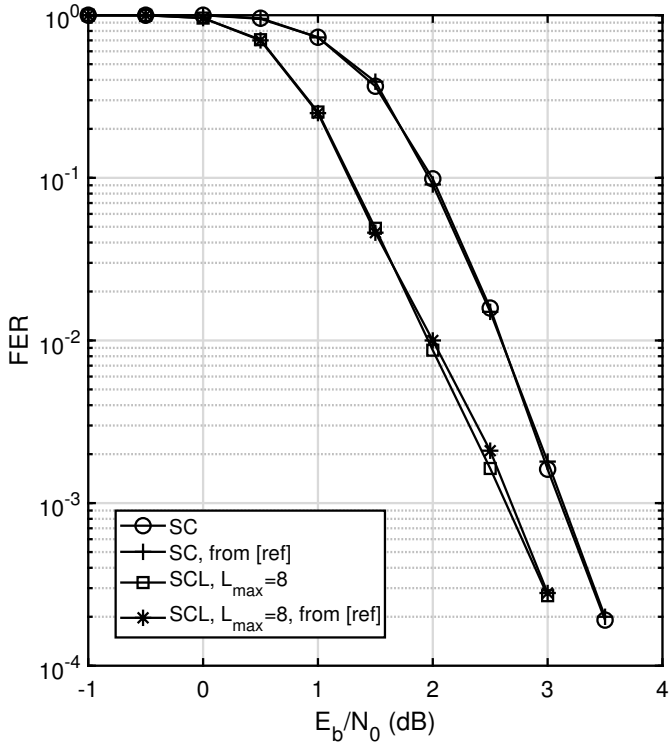

Figure 5. Frame error rate (FER) performance of a $(1024, 512)$ polar code with successive cancellation (SC) and successive cancellation list (SCL) decoders over an additive white Gaussian noise (AWGN) channel and comparison with the results from ref. [60] (marked as [ref]).

4.3. Simulation Results for the Multi-Way Relaying System

We consider four different cases based on the terminals' knowledge of the relays' transmission: (a) the ideal case when all relays transmit; (b) the case when the terminals do not know which relay transmits (case 1); (c) the case when the terminals know which relay transmits (case 2); (d) the case when the terminals do not know which relay transmits, but they use the hard threshold method. In (a), all the terminal–relay transmissions are perfect, and the relays detect all the signals correctly and hence transmit continuously. In (b), although some relays remain silent, the terminals assume the relays always transmit, and all channel LLRs are calculated using (40). In (c), the terminals know which relays transmit and modify all the channel LLRs corresponding to the relays that do not transmit based on (45). In (d), the terminals employ the hard threshold technique to modify the channel LLRs corresponding to the relay signals that do not pass the threshold.

In this work, we consider equal power allocation to all nodes and hence assume unity transmission power $P = 1$ in all simulations. For each bit error rate (BER) point, we simulate at least 1000 randomly generated codewords with independent channel fading realizations and collect at least 500 bit errors. The list size for SCL decoding is set to $L_{max} = 8$. The bit energy E_b is related to the transmission power through the following:

$$E_b = P \cdot \frac{N}{K} \tag{50}$$

The BER performance of a system with five terminals and three relays employing a $(8, 5)$ polar code with SC decoding is shown in Figure 6. The performance results for uncoded DBPSK transmission over a Rayleigh fading channel and a polar code with ML decoding are also included as references. We see that SC decoding achieves the same diversity order as ML decoding. When all the relays transmit, the error performance of SC decoding is very close to the performance of ML decoding. In the non-ideal case 1, we see that SC decoding provides a small advantage over ML decoding, showing that it enjoys a robustness to intermittent relay transmissions. At a BER of 10^{-5}, the performance gap between SC and ML decoding in case 1 is about 0.8 dB. For case 2, when the terminals know which relays transmit, the performance of ML and SC decoding becomes essentially the same. In summary, the error performance of polar codes with SC decoding is very close to ML decoding for short polar codes. The performance with SCL decoding for our multi-way relaying system with such short polar codes is essentially the same as with SC decoding; hence, we do not include these results. We will see that with longer polar codes, SCL decoding provides performance advantages over SC decoding.

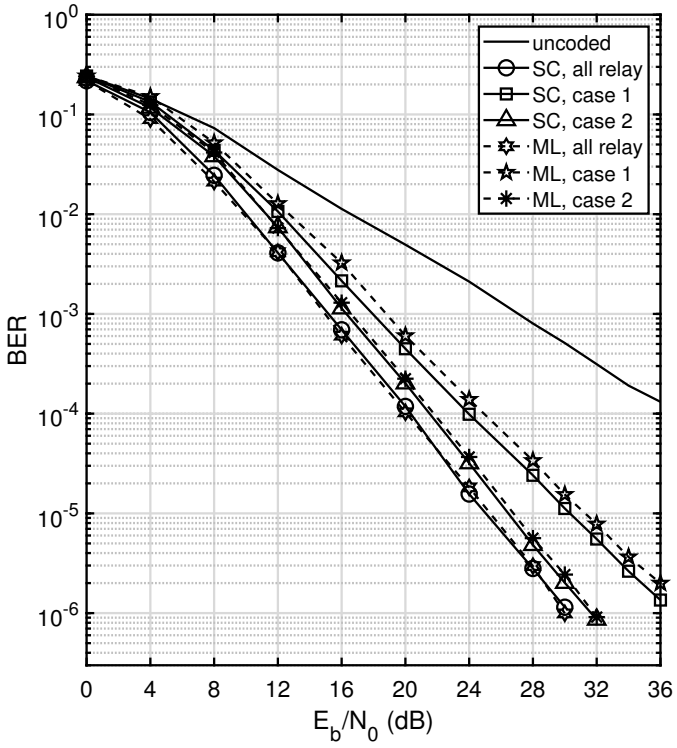

Figure 6. Bit error rate (BER) performance of a $(8, 5)$ polar code with the successive cancellation (SC) and maximum likelihood (ML) decoders.

The BER performance of three longer polar codes with a rate of 0.8125, when used in our multi-way relaying system with all relays transmitting, is shown in Figure 7. All the codes have a significant performance gain compared to the uncoded scheme. At a BER of 10^{-5}, with SC decoding, the $(512, 416)$ code has a performance gain of 2.5 dB compared to the $(128, 104)$ code. With SCL decoding, the performance gain increases to 4 dB. This

suggests that a longer polar code can provide better error performance in our muli-way relaying system. Furthermore, when comparing SC decoding with SCL decoding, for the same code, we see a significant advantage of the later in the form of coding gains in the range of 1.5–3 dB. It is to be noted that the multi-way relaying system employing the $(512, 416)$ code can support 416 users, and the one employing the $(128, 104)$ code can support 104 users. This indicates the ability of the multi-way relaying system using polar codes to support a large number of users, similar to the system in ref. [12] that uses LDPC codes.

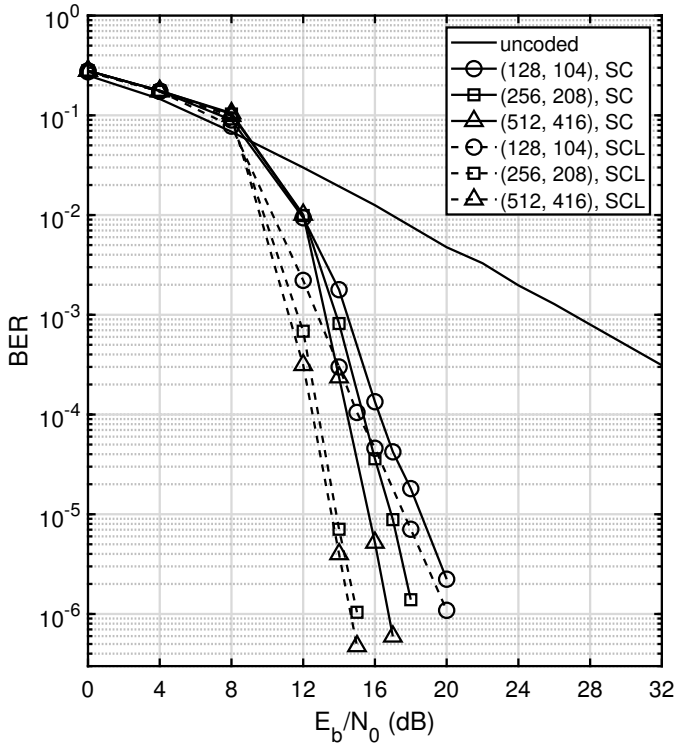

Figure 7. Bit error rate (BER) performance of three long polar codes when all relays transmit.

The BER performance of a $(512, 416)$ polar code with SC and SCL decoding is illustrated in Figure 8 and Figure 9, respectively. Compared to the $(8, 5)$ polar code, the $(512, 416)$ polar code provides a more significant performance gain with both decoding methods over the uncoded scheme in all cases. The SCL decoding method has a better performance of about 2 dB to achieve a BER of 10^{-6} in all four cases compared to SC decoding. The results when the thresholding technique is employed at user terminals are also included in Figures 8 and 9. It is seen that with the thresholding technique, the performance loss with respect to case 2 is reduced from 4 dB to about 1.7 B at a BER of 10^{-6}, demonstrating the effectiveness of this practical approach.

The required E_b/N_0 to achieve a BER of 10^{-6} for the $(512, 416)$ polar code is presented in Table 7. This table also presents similar results for various LDPC codes employing log-BP decoding from [12]. The $(437, 361)$ LDPC code is constructed using the method given in ref. [63]. All the codes have comparable codeword lengths and rates equal or higher than 0.8. In the ideal case when all the relays transmit, the $(512, 416)$ polar code with SCL decoding can achieve a better performance than the two LDPC codes with log-BP decoding. This illustrates the effectiveness of polar codes with SCL decoding for our system when all relays transmit. In the other three non-ideal cases, the polar code with SCL decoding also achieves a performance gain of about 2 dB compared to the $(480, 400)$ LDPC code. In these cases, the BER performance with SC decoding is better than or comparable to the $(480, 400)$ LDPC code. However, the polar code with SCL decoding has a performance loss of about 1.6 dB compared to the $(437, 361)$ LDPC code in these three cases. This is because

the relays of the polar code system have larger relevant group sizes. The average relevant group size of the relays in the $(512, 416)$ polar code system is 69, while the average group size is only 19 for the $(437, 361)$ LDPC code system. With a larger relevant group, for the same E_b/N_0, the relays have a higher probability of detecting a wrong symbol and hence remain silent. This explains the performance degradation of polar codes in non-ideal cases when compared to LDPC codes with a smaller average group size. Although there is a small performance gap between the polar codes and some LDPC codes, the low decoding complexity analyzed in Section 3 makes polar codes competitive for application in our system. A specific construction method for polar codes that also takes into account the relays' average group sizes could result in even better performance.

Table 7. Required E_b/N_0 to achieve a BER of 10^{-6} for polar and low-density parity check (LDPC) codes.

	Rate	All Relay	Case 2	Add Threshold	Case 1
(512, 416) polar, SC	0.8125	17.1 dB	24 dB	25.4 dB	28.3 dB
(512, 416) polar, SCL	0.8125	14.7 dB	22 dB	23.8 dB	26 dB
(480, 400) LDPC	0.8	15.3 dB	22.8 dB	26 dB	28.2 dB
(437, 361) LDPC	0.826	15.2 dB	20.4 dB	22.1 dB	24.5 dB

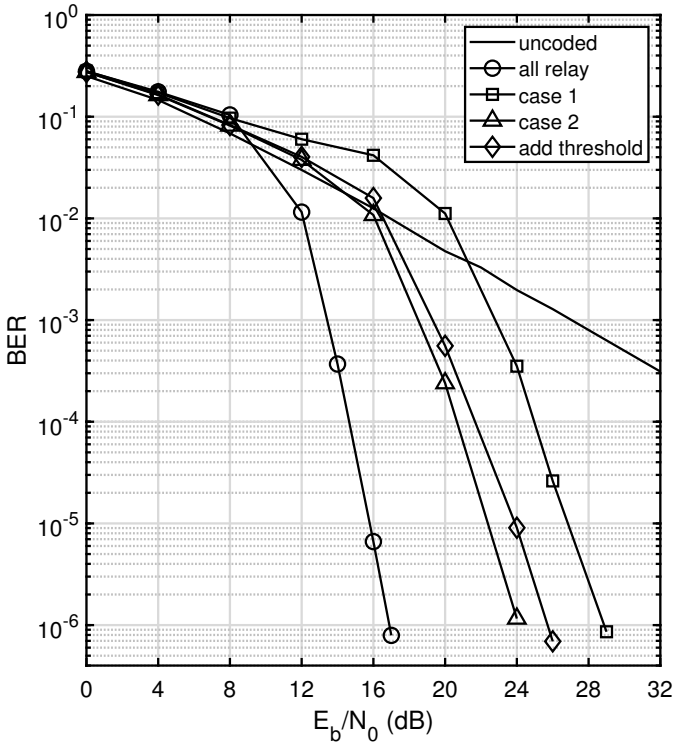

Figure 8. Bit error rate (BER) performance of a $(512, 416)$ polar code with successive cancellation (SC) decoding.

It was observed in [35] that systematic polar codes have a better BER performance compared to non-systematic polar codes. To test the effects of systematic polar encoding in our multi-way relaying system, we first generate the information bits of polar codes $\mathbf{m}_A$, then the terminal bits $\mathbf{m}_T$ are obtained from (36). The BER performance of $\hat{\mathbf{m}}_A$ and $\hat{\mathbf{m}}_T$ for the $(512, 416)$ polar code with SC decoding is presented in Figure 10, and the performance with SCL decoding is presented in Figure 11. The curves corresponding to $\hat{\mathbf{m}}_T$ and $\hat{\mathbf{m}}_A$ are marked with "Ter." and "polar", respectively. In all cases, $\hat{\mathbf{m}}_T$ results in a better error performance compared to $\hat{\mathbf{m}}_A$. The performance advantage of using systematic codes over

equivalent non-systematic codes is in the range of 0.8–1.5 dB. This indicates that our system maintains the performance advantages of systematic encoding for polar codes.

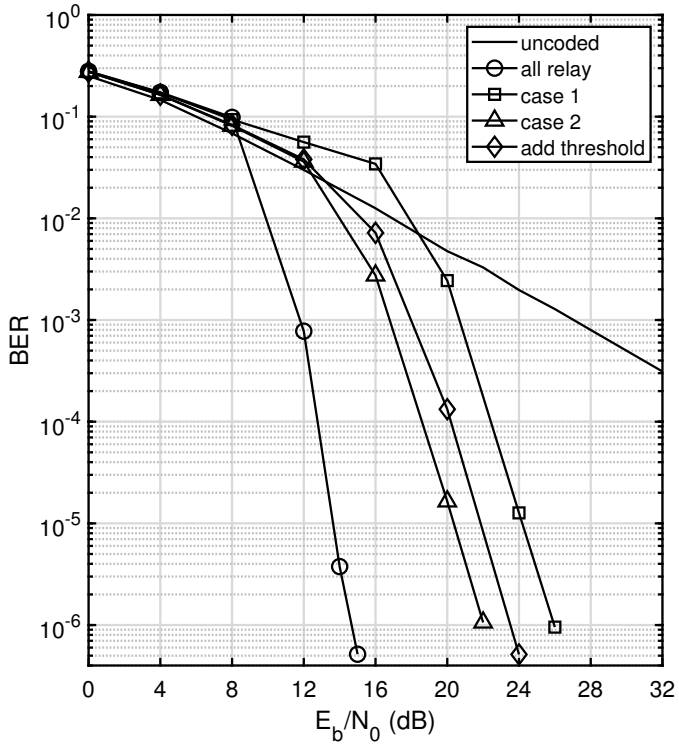

Figure 9. Bit error rate (BER) performance of a $(512, 416)$ polar code with successive cancellation list (SCL) decoding.

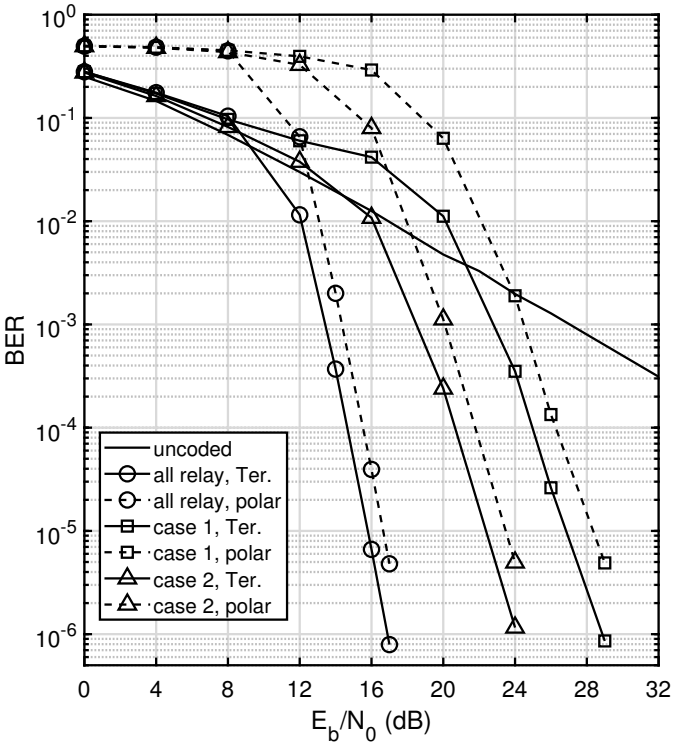

Figure 10. Bit error rate (BER) comparison of $\hat{\mathbf{m}}_T$ and $\hat{\mathbf{m}}_A$ of a $(512, 416)$ polar code with successive cancellation (SC) decoding.

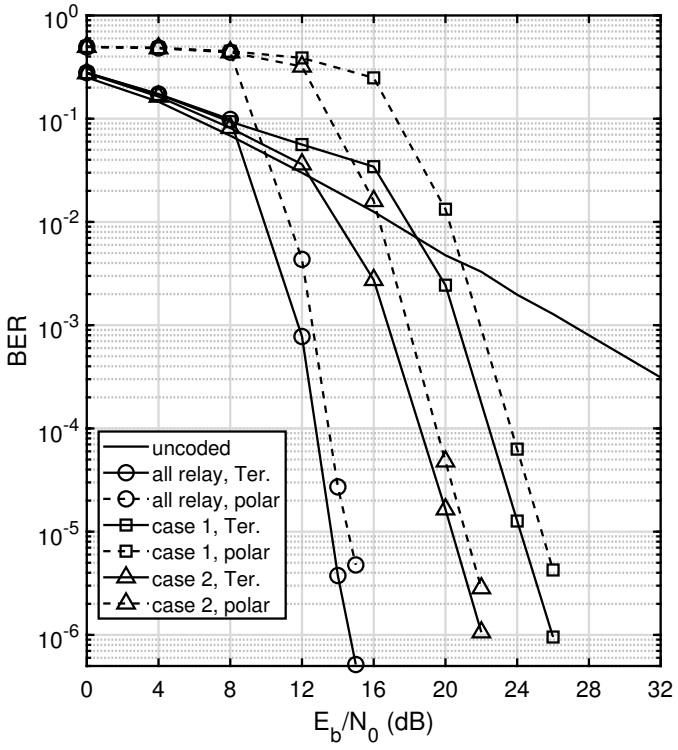

Figure 11. Bit error rate (BER) comparison of $\hat{\mathbf{m}}_T$ and $\hat{\mathbf{m}}_A$ of a $(512, 416)$ polar code with successive cancellation list (SCL) decoding.

5. Conclusions

This paper considers polar codes with DBPSK when used as network codes in multi-way relaying. The use of DBPSK bypasses the need for channel estimation at the receiver side in such systems. This system can be viewed as a systematic linear block code. We present a methodology of using equivalent systematic polar encoding in this system, as well as the the SC and SCL decoding algorithms. Furthermore, this paper also considers the encoding and decoding complexities of the system for linear block codes with ML decoding, LDPC codes with log-BP decoding, and polar codes with SC and SCL decoding. It is shown that polar codes with SC or SCL decoding have a much lower complexity than LDPC codes with log-BP decoding, making them attractive for practical multi-way relaying. We use computer simulations to assess the error rate performance of multi-way relaying employing polar codes with different code lengths and rates. Monte-Carlo simulation results indicate that the system employing polar codes has a significant performance gain compared to an uncoded scheme. For short polar codes, SC and SCL decoding can achieve an error performance that is close to ML decoding. For longer polar codes, the error performance is comparable to LDPC codes with log-BP decoding. For practical applications, we consider a hard threshold technique at the terminals to determine whether a relay transmits. This technique can efficiently reduce the performance loss with respect to the ideal case when a terminal knows when a relay transmits with SC and SCL decoding. When compared with the use of LDPC codes in a multi-way relaying system employing log-BP decoding, polar codes provide similar performance gains. In some cases when the LDPC codes have relevant groups of terminals of small sizes, and hence are more suitable for multi-way relaying, polar codes show a small performance loss of about 1.7 dB in practical cases. Notice that the polar codes we considered in this paper are standard and not specifically designed for multi-way relaying. It is expected that polar codes that are specifically designed for multi-way relaying could provide further performance gains; hence, this topic is of considerable interest for further research. In particular, multi-kernel polar codes offer extra flexibility that could be very appealing for multi-way relaying applications. Even with the standard binary polar codes we used in this work, the advantages of low-complexity

decoding offset the small losses and make polar codes a practical coding technique for multi-way relaying, which is competitive to LDPC codes. While we consider polar codes in this paper, the technique of using a systematic equivalent code for transmission and then a corresponding non-systematic code with structural features that allows for simplified decoding for information retrieval can be used with any linear block code. This method increases the class size of linear block codes that can be used as network codes in multi-way relaying to also include non-systematic codes.

Author Contributions: Conceptualization H.L.; methodology H.L.; software R.J.; investigation R.J. and H.L.; writing—first draft R.J. and H.L.; writing—review and editing, H.L.; supervision, H.L.; funding H.L. All authors have read and agreed to the published version of the manuscript.

Funding: This research was supported by grant RGPIN-2016-03647 awarded by the Natural Sciences and Engineering Research Council of Canada (NSERC).

Data Availability Statement: The original contributions presented in the study are included in the article, further inquiries can be directed to the corresponding author.

Conflicts of Interest: The authors declare no conflicts of interest.

References

1. Silva, B.M.C.; Rodriguess, J.J.P.C.; Kumar, N.; Han, G. Cooperative strategiesi for challenged networks and applications: A survey. *IEEE Syst. J.* **2020**, *11*, 2749–2760. [CrossRef]
2. Ahmed, E.; Gharavi, H. Cooperative vehicular networking: A survey. *IEEE Trans. Intell. Transp. Syst.* **2018**, *19*, 996–1014. [CrossRef] [PubMed]
3. Sharma, S.; Mishra, A.K.; Kumar, M.H.; Deka, K.; Bhatia, V. Intelligent Reflecting Surfaces (IRS)-Enhanced Cooperative NOMA: A Contemporary Review. *IEEE Access* **2024**, *12*, 82168–82191. [CrossRef]
4. Liu, P.; Wang, J.; Ma, K.; Guo, Q. Joint Cooperative Computation and Communication for Demand-Side NOMA-MEC Systems With Relay-Assisted in Smart Grid Communications. *IEEE Internet Things J.* 2024, *early access*. [CrossRef]
5. Zhao, M.; Ye, N.; Ouyang, Q.; Jin, Y.; Jin, Y.; Zhao, L. Multi-Satellite Cooperative Communication: Exploiting Time Asynchrony in Non-Orthogonal Transmissions. *IEEE Trans. Veh. Technol.* **2023**, *72*, 6868–6873. [CrossRef]
6. Mach, P.; Becvar, Z. Device-to-device relaying: Optimization, performance perespectives, and open challenges towards 6G networks. *IEEE Commun. Tutor.* **2022**, *24*, 1336–1393. [CrossRef]
7. Zhang, J.; Leib, H. Bidirectional selective detect-and-forward (DetF) multi-relay systems with regularized WDFDC receivers. *IEEE Access* **2023**, *11*, 143212–143229. [CrossRef]
8. Ropokis, G.A.; Bithas, P.S. Wireless Powered Relay Networks: Rate Optimal and Power Consumption-Aware WPT/SWIPT. *IEEE Trans. Veh. Technol.* **2022**, *71*, 8574–8590. [CrossRef]
9. Tang, S.; He, K.; Chen, L.; Fan, L.; Lei, X.; Hu, R.Q. Collaborative Cache-Aided Relaying Networks: Performance Evaluation and System Optimization. *IEEE J. Sel. Areas Commun.* **2023**, *41*, 706–719. [CrossRef]
10. Gunduz, D.; Yener, A.; Goldsmith, A.; Poor, H.V. The multiway relay channel. *IEEE Trans. Inf. Theory* **2012**, *59*, 51–63. [CrossRef]
11. Kramer, G.; Gastpar, M.; Gupta, P. Cooperative strategies and capacity theorems for relay networks. *IEEE Trans. Inf. Theory* **2005**, *51*, 3037–3063. [CrossRef]
12. Hou, X.; Leib, H. A Network Linear Block Coding Approach to Selective Detect-and-Forward Multi-Way Relaying with Differential Modulation. *IEEE Trans. Wirel. Commun.* **2020**, *19*, 5749–5764. [CrossRef]
13. Yuan, J.; Li, Y.; Chu, L. Differential modulation and relay selection with detect-and-forward cooperative relaying. *IEEE Trans. Veh. Technol.* **2009**, *59*, 261–268. [CrossRef]
14. Woradit, K.; Quek, T.Q.; Suwansantisuk, W.; Wymeersch, H.; Wuttisittikulkij, L.; Win, M.Z. Outage behavior of selective relaying schemes. *IEEE Trans. Wirel. Commun.* **2009**, *8*, 3890–3895. [CrossRef]
15. Ahlswede, R.; Cai, N.; Li, S.Y.; Yeung, R.W. Network information flow. *IEEE Trans. Inf. Theory* **2000**, *46*, 1204–1216. [CrossRef]
16. Zhu, F.; Zhang, C.; Zheng, Z.; Farouk, A. Practical metwork coding technologies and softwarization in wireless networks. *IEEE Internet Things J.* **2021**, *8*, 5211–5218. [CrossRef]
17. Nguyen, H.V.; Ng, S.X.; Liang, W.; Xiao, P.; Hanzo, L. A network-coding aided road-map of large-scale near-capacity cooperative communications. *IEEE Access* **2018**, *6*, 21592–21620. [CrossRef]
18. Heidarpour, A.R.; Ardakani, M.; Tellambura, C.; Uysal, M. Network-Coded Cooperative Systems in Cognitive Radio Networks. *IEEE Trans. Wirel. Commun.* **2022**, *21*, 11011–11023. [CrossRef]
19. Mohammed, A.H.; Dai, B.; Huang, B.; Azhar, M.; Xu, G.; Qin, P.; Yu, S. A survey and tutorial on wireless relay network protocols based on network coding. *J. Netw. Comput. Appl.* **2013**, *36*, 593–610. [CrossRef]
20. Pan, H.; Chan, T.T.; Leung, V.C.M.; Li, J. Age of Information in Physical-Layer Network Coding Enabled Two-Way Relay Networks. *IEEE Trans. Mob. Comput.* **2023**, *22*, 4485–4499. [CrossRef]

21. Zhou, Q.F.; Li, Y.; Lau, F.C.M.; Vucetic, B. Decode-and-Forward Two-Way Relaying with Network Coding and Opportunistic Relay Selection. *IEEE Trans. Commun.* **2010**, *58*, 3070–3076. [CrossRef]
22. Chaaban, A. Multi-way communication:An Information Theoretic Perspective. *NOW Essence Knowl.* **2015**, *12*, 185–371.
23. Arikan, E. Channel polarization: A method for constructing capacity-achieving codes for symmetric binary-input memoryless channels. *IEEE Trans. Inf. Theory* **2009**, *55*, 3051–3073. [CrossRef]
24. Gazi, O. *Polar Codes: A Non-Trivial Approach to Channel Coding*; Spinger Nature: Berlin, Germany, 2019.
25. Berrou, C.; Glavieux, A.; Thitimajshima, P. Near Shannon limit error-correcting coding and decoding: Turbo-codes. 1. In Proceedings of the ICC'93-IEEE International Conference on Communications, Geneva, Switzerland, 23–26 May 1993; Volume 2, pp. 1064–1070.
26. Gallager, R. Low-density parity-check codes. *IRE Trans. Inf. Theory* **1962**, *8*, 21–28. [CrossRef]
27. Bioglio, V.; Condo, C.; Land, I. Design of polar codes in 5G new radio. *IEEE Commun. Surv. Tutor.* **2021**, *23*, 29–40. [CrossRef]
28. Sun, H.; Viterbo, E.; Dai, B.; Liu, R. Fast Decoding of Polar Codes for Digital Broadcasting Services in 5G. *IEEE Trans. Broadcast.* **2024**, *70*, 731–738. [CrossRef]
29. Rowshan, M.; Qiu, M.; Xie, Y.; Gu, X.; Yuan, J. Channel Coding Toward 6G: Technical Overview and Outlook. *IEEE Open J. Commun. Soc.* **2024**, *5*, 2585–2685. [CrossRef]
30. Tal, I.; Vardy, A. List decoding of polar codes. *IEEE Trans. Inf. Theory* **2015**, *61*, 2213–2226. [CrossRef]
31. Soliman, T.; Yang, F.; Ejaz, S. Decode and forward polar coding for Half-duplex two-relay channels based on multilevel construction. *Int. J. Electron.* **2017**, *104*, 539–554. [CrossRef]
32. Blasco-Serrano, R.; Thobaben, R.; Andersson, M.; Rathi, V.; Skoglund, M. Polar codes for cooperative relaying. *IEEE Trans. Commun.* **2012**, *60*, 3263–3273. [CrossRef]
33. Zhan, Q.; Du, M.; Wang, Y.; Zhou, F. Half-duplex relay systems based on polar codes. *IET Commun.* **2014**, *8*, 433–440. [CrossRef]
34. HADI, A.S.H.; Orhan, G. The Research and Design of Multi Relays in Cooperative Communication System Based on Polar Codes. *Cankaya Univ. J. Sci. Eng.* **2021**, *18*, 117–124.
35. Arikan, E. Systematic polar coding. *IEEE Commun. Lett.* **2011**, *15*, 860–862. [CrossRef]
36. Wang, X.; Zhang, Z.; Li, J.; Wang, Y.; Cao, H.; Li, Z.; Shan, L. An optimized encoding algorithm for systematic polar codes. *EURASIP J. Wirel. Commun. Netw.* **2019**, *2019*, 193. [CrossRef]
37. Vangala, H.; Hong, Y.; Viterbo, E. Efficient algorithms for systematic polar encoding. *IEEE Commun. Lett.* **2015**, *20*, 17–20. [CrossRef]
38. Li, L.; Zhang, W. On the encoding complexity of systematic polar codes. In Proceedings of the 2015 28th IEEE International System-on-Chip Conference (SOCC), Beijing, China, 8–11 September 2015; pp. 415–420.
39. Sarkis, G.; Giard, P.; Vardy, A.; Thibeault, C.; Gross, W.J. Fast polar decoders: Algorithm and implementation. *IEEE J. Sel. Areas Commun.* **2014**, *32*, 946–957. [CrossRef]
40. Sarkis, G.; Tal, I.; Giard, P.; Vardy, A.; Thibeault, C.; Gross, W.J. Flexible and low-complexity encoding and decoding of systematic polar codes. *IEEE Trans. Commun.* **2016**, *64*, 2732–2745. [CrossRef]
41. Fujiwara, S.; Ochiai, H. A Flexible Polar Decoding Architecture With Adjustable Latency and Reliability. *IEEE Open J. Commun. Soc.* **2024**, *5*, 951–964. [CrossRef]
42. Shen, Y.; Zhou, W.; Huang, Y.; Zhang, Z.; You, X.; Zhang, C. Fast Iterative Soft-Output List Decoding of Polar Codes. *IEEE Trans. Signal Process.* **2022**, *70*, 1361–1376. [CrossRef]
43. Lee, C.; Park, C.; Back, S.; Oh, W. Low Complexity Early Stopping Belief Propagation Decoder for Polar Codes. *IEEE Access* **2024**, *12*, 72098–72104. [CrossRef]
44. Timokhin, I.; Ivanov, F. Sequential polar decoding with cost metric threshold. *Appl. Sci.* **2024**, *14*, 1847. [CrossRef]
45. Han, S.; Kim, B.; Chung, J.; Ha, J. Improved Automorphism Ensemble Decoder for Polar Codes. *IEEE Commun. Lett.* 2024, *early access*. [CrossRef]
46. Zhou, Y.; Qin, Z.; Wang, Z. Efficient Soft-Cancellation Flip Decoding of Polar Codes. *IEEE Commun. Lett.* 2024, *early access*. [CrossRef]
47. Trifonov, P.V. Design and decoding of polar codes with large kernels: A survey. *Probl. Inf. Transm.* **2023**, *59*, 22–40. [CrossRef]
48. Biglieri, E.; Proakis, J.; Shamai, S. Fading channels: Information-theoretic and communication aspects. *IEEE Trans. Inf. Theory* **1998**, *44*, 2619–2692. [CrossRef]
49. Himson, T.; Siriwongpairat, W.P.; Su, W.; Liu, L.J.R. Differential modulation for multinode cooperative communication. *IEEE Trans. Signal Proc.* **2008**, *56*, 2941–2956.
50. Dai, G.; Leib, H. Detect-and-forward multirelay systems with decision-feedback differentially coherent receivers. *IEEE Trans. Wirel. Commun.* **2016**, *15*, 1267–1282. [CrossRef]
51. Wymeersch, H.; Steendam, H.; Moeneclaey, M. Log-domain decoding of LDPC codes over GF(q). In Proceedings of the 2004 IEEE International Conference on Communications (IEEE Cat. No. 04CH37577), Paris, France, 20–24 June 2004; Volume 2, pp. 772–776.
52. Abbe, E.; Sberlo, O.; Shpilka, A.; Ye, M. Reed-Muller Codes. *Found. Trends Commun. Inf. Theory* **2023**, *20*, 1–156. [CrossRef]
53. Leroux, C.; Tal, I.; Vardy, A.; Gross, W.J. Hardware architectures for successive cancellation decoding of polar codes. In Proceedings of the 2011 IEEE International Conference on Acoustics, Speech and Signal Processing (ICASSP), Prague, Czech Republic, 22–27 May 2011; pp. 1665–1668. [CrossRef]

54. Balatsoukas-Stimming, A.; Parizi, M.B.; Burg, A. LLR-based successive cancellation list decoding of polar codes. *IEEE Trans. Signal Process.* **2015**, *63*, 5165–5179. [CrossRef]
55. Proakis, J.G.; Salehi, M. *Digital Communications*; McGraw-Hill: New York, NY, USA, 2008.
56. Hou, X. A Network Linear Block Coding Approach to Selective Detectand-Forward Multi-Way Relaying. Master's Thesis, Department of Electrical and Computer Engineering, McGill University, Montreal, QC, Canada, 2019.
57. Ji, R. Multi-Way Relaying Systems Based on Network Polar Codes. Master's Thesis, Department of Electrical and Computer Engineering, McGill University, Montreal, QC, Canada, 2023.
58. Zhang, J. Selective Decode-and-Forward Bidirectional Multi-Relay Networks with Regularized Weighted Decision Feedback Differential Coherent Receivers. Master's Thesis, Department of Electrical and Computer Engineering, McGill University, Montreal, QC, Canada, 2017.
59. Vangala, H.; Viterbo, E.; Hong, Y. A comparative study of polar code constructions for the AWGN channel. *arXiv* **2015**, arXiv:1501.02473.
60. Babar, Z.; Egilmez, Z.B.K.; Xiang, L.; Chandra, D.; Maunder, R.G.; Ng, S.X.; Hanzo, L. Polar codes and their quantum-domain counterparts. *IEEE Commun. Surv. Tutor.* **2019**, *22*, 123–155. [CrossRef]
61. 3GPP. Multiplexing and Channel Coding; Technical Specification (TS) 38.212, 3rd Generation Partnership Project (3GPP); 2018; Volume 6. Available online: https://www.etsi.org/deliver/etsi_ts/138200_138299/138212/15.02.00_60/ts_138212v150200p.pdf (accessed on 30 July 2024).
62. Hasan, A.A.; Marsland, I.D. Low complexity LLR metrics for polar coded QAM. In Proceedings of the 2017 IEEE 30th Canadian Conference on Electrical and Computer Engineering (CCECE), Windsor, ON, Canada, 30 April–3 May 2017; pp. 1–4.
63. Suthisopapan, P.; Kupimai, M.; Tongta, R.; Imtawil, V. Design of high-rate LDGM codes. In Proceedings of the 2009 Fourth International Conference on Communications and Networking in China, Xi'an, China, 26–28 August 2009; pp. 1–4.

Disclaimer/Publisher's Note: The statements, opinions and data contained in all publications are solely those of the individual author(s) and contributor(s) and not of MDPI and/or the editor(s). MDPI and/or the editor(s) disclaim responsibility for any injury to people or property resulting from any ideas, methods, instructions or products referred to in the content.